Environmental Science & Technology Letters

Letter

Cite This: Environ. Sci. Technol. Lett. 2019, 6, 119−125

pubs.acs.org/journal/estlcu

Phospholipid Levels Predict the Tissue Distribution of Poly- and Perfluoroalkyl Substances in a Marine Mammal

Clifton Dassuncao,*[,†,‡] Heidi Pickard,[†] Marisa Pfohl,[§] Andrea K. Tokranov,[†] Miling Li,[†] Bjarni Mikkelsen,[∥] Angela Slitt,[§] and Elsie M. Sunderland[†,‡]

[†]Harvard John A. Paulson School of Engineering and Applied Sciences, Harvard University, Cambridge, Massachusetts 02138, United States

[‡]Department of Environmental Health, Harvard T. H. Chan School of Public Health, Harvard University, Boston, Massachusetts 02115, United States

[§]Biomedical and Pharmaceutical Sciences, University of Rhode Island, Kingston, Rhode Island 02881, United States

[∥]Museum of Natural History, Tórshavn, Faroe Islands 188

Supporting Information

ABSTRACT: Exposure to poly- and perfluoroalkyl substances (PFASs) has been linked to many negative health impacts in humans and wildlife. Unlike neutral hydrophobic organic pollutants, many PFASs are ionic and have been hypothesized to accumulate in both phospholipids and protein-rich tissues. Here we investigate the role of phospholipids for PFAS accumulation by analyzing associations among concurrent measurements of phospholipid, total protein, total lipid, and 24 PFASs in the heart, muscle, brain, kidney, liver, blubber, placenta, and spleen of North Atlantic pilot whales (*Globicephala melas*). The sum of 24 PFASs ($\sum_{24}$ PFAS) was highest in the liver [median of 260 ng g^{-1}; interquartile range (IQR) of 216−295 ng g^{-1}] and brain (86.0 ng g^{-1}; IQR of 54.5−91.3 ng g^{-1}), while phospholipid levels were highest in the brain. The relative abundance of PFASs in the brain greatly increases with carbon-chain lengths of ≥10, suggesting shorter-chain compounds may cross the blood−brain barrier less efficiently. Phospholipids were significant predictors of the tissue distribution of the longest-chain PFASs: perfluorodecanesulfonate (PFDS), perfluorododecanoate (PFDoA), perfluorotridecanoate (PFTrA), and perfluorotetradecanoate (PFTA) (r_s = 0.5−0.6). In all tissues except the brain, each 1 mg g^{-1} increase in phospholipids led to a 12−25% increase in the concentration of each PFAS. We conclude that partitioning to phospholipids is an important mechanism of bioaccumulation for long-chain PFASs in marine mammals.

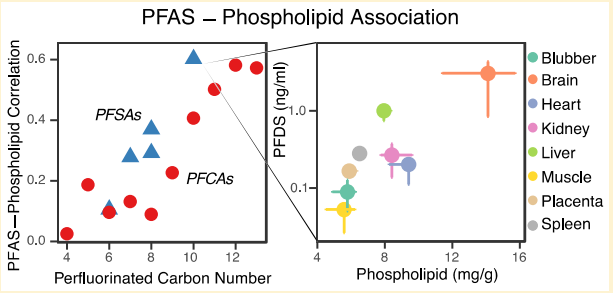

1. INTRODUCTION

Human exposure to poly- and perfluoroalkyl substances (PFASs) has been associated with metabolic disruption, immunotoxicity, and cancer.[1,2] Many PFASs have long environmental lifetimes and bioaccumulate in aquatic food webs.[3,4] As a result, seafood consumption is an important human exposure pathway.[5] Hydrophobic persistent organic pollutants are known to accumulate in neutral storage lipids.[6] However, factors controlling the bioaccumulation and tissue distribution of different PFASs are not fully understood.[7−9]

Perfluoroalkyl acids (PFAAs), an important subclass of PFASs, are anionic under environmentally relevant conditions and accumulate in certain protein-rich tissues such as blood and liver.[10−12] Two mechanisms for PFAA accumulation have been proposed in prior work: (1) partitioning to phospholipids[8,13] and (2) binding to specific proteins.[9] Both phospholipids and PFAAs contain a hydrophilic head and a hydrophobic tail. The phospholipid model proposes that cell membranes, which are composed of phospholipids, act as a significant sink for PFAAs.[13] Phospholipid−water partition coefficients and related proxies thus provide a potential screening metric for bioaccumulation of organic ions.[14−16]

Here we investigate whether the phospholipid content of marine mammal tissues can be used to predict PFAS accumulation. We hypothesize that correlations between phospholipid content and PFAS concentrations will vary on the basis of their functional group and carbon-chain length.[17,18] We further hypothesize that structural proteins and storage lipids act as significant sorption compartments for neutral or semineutral PFASs. We test these hypotheses using concurrent measurements of 24 PFASs, total phospholipids, total lipids, and total protein concentrations across multiple organ tissues in seven North Atlantic pilot whales (*Globicephala melas*). We

Received: January 13, 2019
Revised: February 16, 2019
Accepted: February 20, 2019
Published: February 20, 2019

Downloaded via HARVARD UNIV on March 22, 2019 at 19:37:24 (UTC).
See https://pubs.acs.org/sharingguidelines for options on how to legitimately share published articles.

© 2019 American Chemical Society

DOI: 10.1021/acs.estlett.9b00031
Environ. Sci. Technol. Lett. 2019, 6, 119−125

use these data to better understand factors affecting PFAS accumulation and partitioning among mammalian tissues.

2. MATERIALS AND METHODS

Long-finned pilot whale samples were collected by the Faroese Natural History Museum in the summer of 2016. Samples were stored frozen at −20 °C at the Faroese Museum of Natural History. We subsampled available tissues, including muscle, heart, kidney, liver, brain, and blubber, from each whale. For a subset of whales, placenta (n = 4) and spleen (n = 2) were also collected. Blood samples were not available for analysis, and tissue samples were not exsanguinated prior to being frozen and analyzed.

Tissue samples were analyzed for 24 PFASs at Harvard University following established methods for extraction and quantification of PFASs as previously described by Weber et al.[19] and Zhang et al.[20] Total protein was quantified with a Bio-Rad DC Protein Assay kit.[21] Total protein in these tissues reflects the most prevalent type of protein (structural proteins). Lipid extraction was based on the Folch method.[22] Phospholipid levels were quantified with an EnzyChrom Phopholipid Assay Kit (EPLP-100) from BioAssay Systems. Additional details about PFAS, protein, and phospholipid analyses are available in the Supporting Information.

Repeated tissue measurements within a whale violate assumptions of independence in a traditional regression. Therefore, we developed a mixed-effects regression model (eq S1) to quantify the importance of phospholipids, total protein, and total lipid partitioning for PFAS accumulation. We conducted sensitivity analyses to consider individual tissue level effects related to specific protein binding and membrane permeability. For these analyses, we compared model results using measurements from all tissues to models that removed observations from selected tissue types. This avoids confounding from processes related to specific protein binding in the liver and effects of the blood−brain barrier on accumulation in the brain. Further details of statistical analyses can be found in the Supporting Information.

3. RESULTS AND DISCUSSION

3.1. Tissue Specific Concentrations. Figure 1 shows measured tissue specific concentrations of phospholipids, total protein, total lipids, and the sum of 24 PFASs ($\sum_{24}$ PFAS). Concentrations of the $\sum_{24}$ PFAS do not vary with the same pattern as total protein, total lipid, or phospholipids across tissues (Figure 1 and Table S3). Significantly higher concentrations of $\sum_{24}$ PFAS were found in the liver [median of 260 ng g^{-1}; interquartile range (IQR) of 216−295 ng g^{-1}] than in any other tissue, and the lowest concentrations were present in muscle (20.5 ng g^{-1}; IQR of 12.9−23.9 ng g^{-1}) and blubber (13.9 ng g^{-1}; IQR of 13.3−14.5 ng g^{-1}) (Figure 1A). Levels of phospholipids were significantly higher in the brain than in any other tissue (Figure 1B). Total protein was not statistically different across the liver, kidney, muscle, spleen, and placenta (Figure 1C). Total lipids were significantly higher in blubber than in any other tissue (Figure 1D).

3.2. Variability across PFASs and Tissues. PFOS, FOSA, and PFCAs with 9−14 carbons (C9−C14) were consistently the most abundant PFASs across tissues (Figure 2A). PFOS accounted for 9% of $\sum_{24}$ PFAS in the brain and 18−26% in all other tissues. C9−C14 PFCAs accounted for 39% of $\sum_{24}$ PFAS in blubber and 72% in the brain. PFTrA

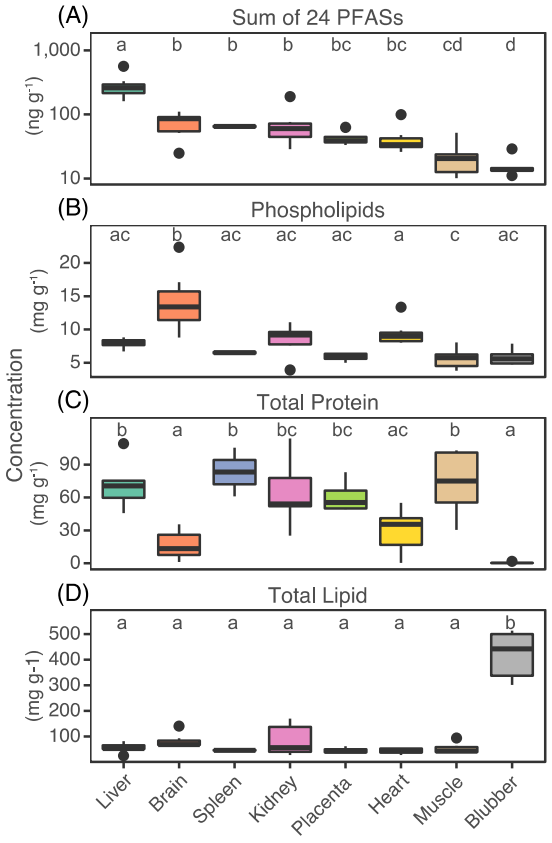

Figure 1. Measured concentrations of (A) the sum of 24 PFASs, (B) phospholipids, (C) total protein, and (D) total lipid in each pilot whale tissue. The dark line within the box represents the median, and box hinges represent the first and third quartiles. The whiskers represent 1.5 times the interquartile range, and black points are outliers. Common letters above each box indicate tissues with no significant difference between group comparisons using Tukey's test.

alone represented 43% in the brain and between 10 and 28% in the remaining tissues. The sulfonate with the longest carbon chain, PFDS, made up 4% of $\sum_{24}$ PFAS in the brain and <1% in other tissues. The contribution of the semineutral precursor FOSA to $\sum_{24}$ PFAS ranged from 7% in liver to 25% in muscle. A higher proportion of C9−C14 PFCAs observed in the brain may reflect differential transport of specific PFASs across the blood−brain barrier and/or differences in the amount and types of binding proteins in cerebral spinal fluid (CSF) compared to whole blood. These findings are consistent with results from Wang et al.[23] that showed varying efficiencies for PFASs crossing the blood−brain barrier in humans, although this study did not reliably detect long-chain compounds.

Figure 2B shows differences in the distribution of individual PFASs based on their carbon-chain length and functional group. Phospholipid levels are highest in the brain. There, the longest-chain compounds (PFDS, PFTrA, and PFTA) are proportionally more abundant than in other tissues (Figure 1). The highest concentrations of C9−C12 PFCAs, PFOS, and FOSA are in the liver. Concentrations in the liver are highest for PFUnDA (C11) and decrease for compounds with shorter and longer carbon chains. An exception to this pattern is PFHxA, which is almost exclusively present in the liver (Figure 2 and Table S3).

The liver contains high concentrations of specific proteins, such as liver fatty acid binding protein (L-FABP). Prior work

DOI: 10.1021/acs.estlett.9b00031
Environ. Sci. Technol. Lett. 2019, 6, 119−125

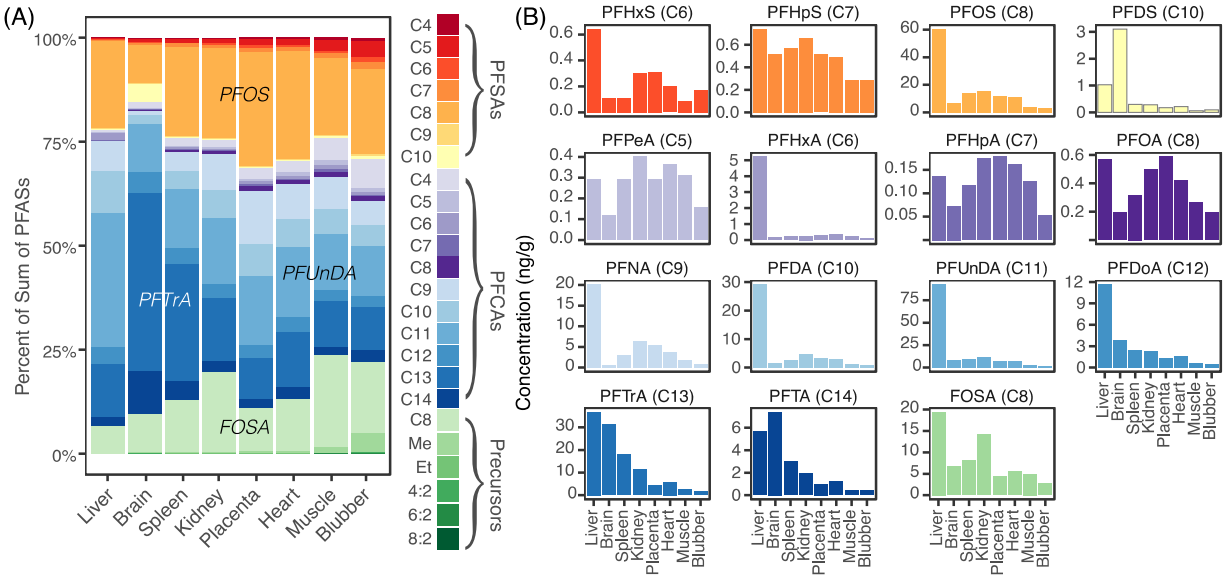

Figure 2. Distribution of PFASs measured in pilot whale tissues. (A) Average composition of 24 PFASs within each tissue. PFCAs and PFSAs are indicated by carbon number (C4−C14), and the precursors FOSA as C8. MeFOSAA is indicated as Me, and EtFOSAA as Et, and fluorotelomer sulfonates are indicated by their carbon numbers. (B) Relative distribution of each PFAS across tissues. Compounds shown in panel A but not in panel B were infrequently detected (<15%).

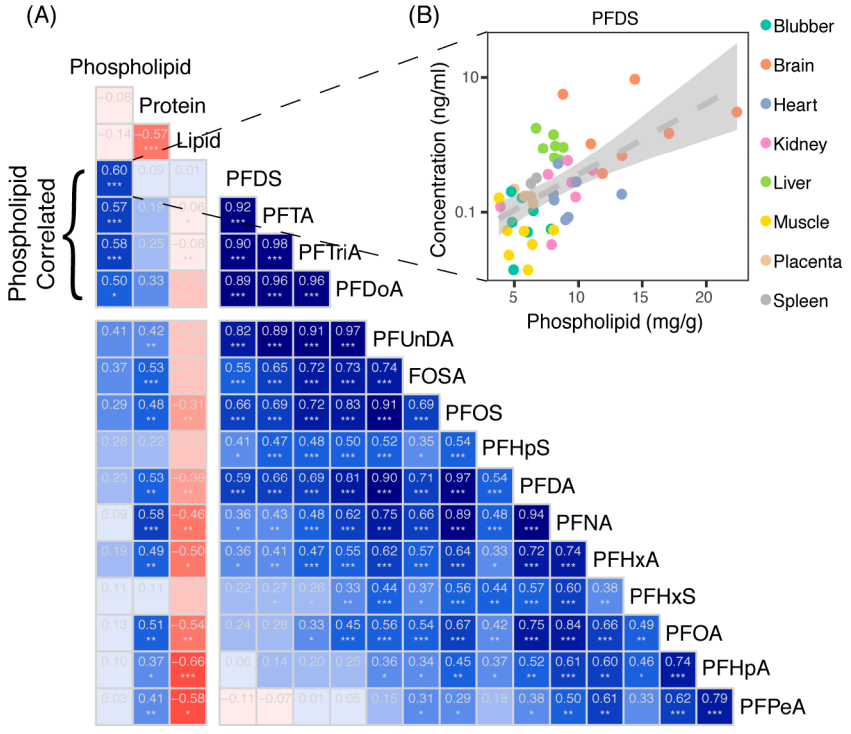

Figure 3. (A) Spearman correlations (r_s) between measured compounds across whale tissues ordered and grouped by degree of correlation. The intensities of blue and red show the strength of positive and negative correlations, respectively. Significant correlations are denoted by asterisks (*p < 0.05; **p < 0.005; ***p < 0.0005). (B) Example of the measured data underlying the correlation between phospholipids and PFDS.

shows L-FABP efficiently binds PFASs.[24−26] Liver is also the site of the production of albumin in mammals, another specific protein that has been associated with PFASs.[27−29] The accumulation of PFHxA in the liver may thus reflect a specific affinity for these proteins. Alternatively, because the liver is the primary site of metabolism, elevated levels of PFHxA in this tissue may represent a high level of exposure to precursor compounds. Urban runoff, wastewater, and aqueous film-forming foams (AFFF) have all been shown to contain a large fraction of precursor compounds that oxidize to PFHxA.[30−33] Quantifying total precursors in ocean water or in tissues may clarify the source of the observed liver levels in marine biota.

3.3. Association among PFASs, Phospholipids, Total Lipid, and Total Protein. Figure 3A shows strong correlations among PFASs with similar chain lengths (i.e., Spearman correlation r_s = 0.98 for PFTA and PFTrA). PFSAs are more correlated with longer PFCAs. For example, the distribution of PFOS was most similar to that of PFDA (r_s =

DOI: 10.1021/acs.estlett.9b00031
Environ. Sci. Technol. Lett. 2019, 6, 119−125

Table 1. Results of Mixed-Effects Regression Models Showing Percent Changes in PFAS Concentration for Each Milliram per Gram Increase in Phospholipid, Protein, or Lipid Concentration

		model with all tissues						model without brain[a]					
PFAS	no. of carbons	PL (%)	*p*	protein (%)	*p*	lipid (%)	*p*	PL (%)	*p*	protein (%)	*p*	lipid (%)	*p*
PFDS	10	26	<0.001	–	–	–	–	20	0.043	–	–	–	–
PFTA	14	22	<0.001	0.9	0.049	–	–	19	<0.001	1.2	0.007	–	–
PFTrA	13	23	<0.001	1.3	0.006	–	–	23	<0.001	1.6	0.001	–	–
PFDoA	12	17	0.001	1.3	0.005	–	–	22	0.017	1.5	0.004	–	–
PFUnDA	11	12	0.025	1.8	0.001	–	–	24	0.025	1.8	0.003	–	–
PFDA	10	–	–	1.7	0.001	–	–	24	0.017	1.7	0.002	–	–
PFOS	8	–	–	1.4	0.002	–	–	25	0.007	1.4	0.003	–	–
FOSA	8	8.5	0.005	1.3	<0.001	–	–	19	<0.001	1.3	<0.001	–	–
PFNA	9	–	–	2.0	<0.001	–	–	23	0.007	1.6	0.001	–	–
PFOA	8	–	–	1.0	0.001	–	–	12	0.003	0.6	0.005	–	–
PFHxS	6	–	–	–	–	–	–	19	0.034	–	–	–	–
PFHpA	7	–	–	1	<0.001	–	–	–	–	–	–	−0.3	<0.001
PFHxA	6	–	–	1	0.025	–	–	22	0.023	–	–	–	–
PFPeA	5	–	–	1	0.006	–	–	15	<0.001	–	–	–	–

[a]Performed as a sensitivity analysis to test for confounding by brain specific processes such as the effects of the blood−brain barrier.

0.97), a PFCA with two more carbons, and PFDS exhibited the highest correlation with PFTA, which has four more carbons. This is consistent with the current understanding of the varying affinities of PFSAs for partitioning to phospholipid bilayers compared to PFCAs.[18,33]

The longest-chain perfluoroalkyl acids (PFDS, PFDoA, PTrDA, and PFTA) are significantly correlated with phospholipid content (r_s = 0.50−0.60) (Figure 3A). The most highly correlated compound is PFDS, and this relationship is driven by the high phospholipid levels measured in the brain (Figure 3B). A pattern of decreasing correlation with phospholipid levels with shorter-chain PFASs is also observed (Figure 3A). By contrast, most other compounds were significantly correlated with total protein levels. The strongest positive association with protein content was observed for PFNA (r_s = 0.58). The negative correlation between PFASs and lipid content is driven by low PFAS concentrations but high lipid levels in blubber. Different patterns of correlation across compounds point toward multiple mechanisms of accumulation.

Results from mixed regression models (Table 1) show a pattern consistent with the univariate correlations (Figure 3A). The best model with all tissues shows significant associations with phospholipids for C11−C14 PFCAs, PFDS, and FOSA. The strongest association is with PFDS. For each 1 mg g^{-1} increase in phospholipids, there is a 26% increase in PFDS. Comparatively weaker but significant protein associations are apparent across all compounds except PFHxS (1−2% change in PFAS per milligram per gram increase in protein). No model retained significant lipid association.

PFASs with more carbons are more strongly associated with tissue phospholipid content (Figure 3A and Table 1, model with all tissues). PFDS and PFOS are more strongly associated with phospholipids than their corresponding PFCAs. These patterns are consistent with accumulation that is driven by both the hydrophobic forces from the fluorinated tail and ionic forces from the polar headgroup. These patterns are also similar to the relative bioaccumulation potential reported for different PFASs,[3] suggesting that phospholipid partitioning may be a primary mechanism of bioaccumulation in marine mammals.

3.4. Longest-Chain Compounds Pass the Blood−Brain Barrier. Because PFAS measurements in the brain appear to be driving the correlation with phospholipids (Figure 3B), we removed these observations as an analysis of sensitivity for the mixed-effects regression model (Table 1). The resulting association with phospholipids is significant for all compounds except PFHpA (Table 1, model without brain). This model indicates each 1 mg g^{-1} increase in phospholipids leads to a 12−25% increase in PFAS concentration (Table 1). These results demonstrate the robustness of the phospholipid association for the longest-chain PFASs and suggest that differing patterns of accumulation in brain tissue are confounding the association for the shorter-chain PFASs.

The effect of the blood−brain barrier on PFAS accumulation is captured by differences between the two mixed-effect regression models (with and without brain measurements, Table 1). Compounds with <10 perfluorinated carbons are not associated with phospholipids in the model that includes brain measurements. This suggests that the shorter-chain compounds may not efficiently cross the blood−brain barrier and/or there are significant differences in the types and levels of proteins in the brain that bind PFASs compared to other tissues. These results are consistent with elevated levels of long-chain PFASs that have been observed in the brain of other mammals.[11,12] Our modeling approach suggests C12−C14 PFCAs and PFDS may cross the blood−brain barrier through a process mediated by an association with phospholipids.

These results have important implications for the mechanisms of accumulation and toxicity of long-chain PFASs. For example, in vitro studies have shown that PFOS can increase the permeability of the blood−brain barrier.[34] A study of paired cerebral spinal fluid and serum samples in humans found that penetration of PFCAs across the blood−brain barrier increased with chain length.[23] An increase in carbon-chain length has also been associated with a decrease in neuron viability in rats[35] and altered brain activity in polar bears.[36]

3.5. Implications for Bioaccumulation. In the simplest case, without considering metabolism and kinetics, the ability of a tissue to acquire a compound can be described by its sorption capacity, K_{BW} (eq 1).[37−39] The total sorption capacity will be dependent on (1) the relative volume fractions of each sorption compartment [storage lipids (f_{SL}), phospholipids

DOI: 10.1021/acs.estlett.9b00031
Environ. Sci. Technol. Lett. 2019, 6, 119−125

(f_{PL}), structural proteins (f_{SP}), and binding proteins (f_{BP})] and (2) the affinity of each compound for each sorption compartment described by their respective partition coefficients ($K_{SL,W}$, $K_{PL,W}$, $K_{SP,W}$, and $K_{BP,W}$). For hydrophobic POPs, the octanol−water partition coefficient, K_{OW}, is used as a surrogate for $K_{SL,W}$ and dominates eq 1.

$$K_{BW} = C_{PFAS}/C_{water} = K_{SL,W}f_{SL} + K_{PL,W}f_{PL} + K_{SP,W}f_{SP} + K_{BP,W}f_{BP} + f_W \quad (1)$$

The regression model we developed in this study (eq S1) parallels that of eq 1. We can therefore compare patterns in the regression coefficients with distribution coefficients estimated empirically by other means. Experimental measurements confirm that PFASs can be incorporated into phospholipid bilayers and that the strength of these interactions differs according to carbon-chain length and functional group.[18,33,40] In fact, all estimates of $K_{PL,W}$ increase with carbon-chain length,[13,17,38] which is consistent with the increase in the level of association with chain length observed in this study (Figure 3).

Several studies report a curvilinear relationship between chain length and protein water association constants (K_{PW}). Literature estimates of K_{PW} based on albumin affinity show peak binding affinity in PFCAs with anywhere from seven (PFHpA) to nine (PFNA) carbons.[27−29] A similar peak in protein association for PFNA is observed in this study, although the protein measurement reported here represents total proteins (Figure 3). Albumin is found in the blood, and while we were unable to obtain paired blood samples from these whales, associations with L-FABP show a similar nonmonotonic relationship between chain length and binding affinity with a maximum occurring at 11 carbons (PFUnDA).[28] Figure 2B shows the relative proportion of PFASs in liver peaks at PFUnDA, which is consistent with the binding affinities for L-FABP.

PFASs can also be transported by organic anion transporters (OATs) and organic anion-transporting polypeptides (OATPs), which control reabsorption of organic anions from urine in the kidney.[41−43] These transporter proteins as well as Na^+/taurocholate co-transporting polypeptide (NTCP) have also been shown to be important for mediating uptake of PFASs in the liver.[44] In contrast, the brain has very low levels of transporter proteins and may therefore reflect PFASs that are more passively permeable. Variability in PFAS affinities for specific proteins may therefore account for the additional variability not explained by the phospholipid associations modeled in Table 1 and should be explored in future work.

The protein measures presented here represent total protein and do not distinguish among specific proteins that have been associated with PFASs. On a related note, the presence of residual whole blood in the tissue samples may obscure the interpretation of some of the results such as the lack of a significant difference in total proteins across many of the tissues (Figure 1C) or the distinct results observed for brain measurements (Table 1). Future studies may wish to concurrently measure specific proteins and PFASs to further clarify the role of proteins. Despite these limitations, the significant associations with phospholipids observed in this study point to their importance for accumulation of PFASs.

Our data are consistent with both protein and phospholipid accumulation for PFASs and can be used to develop a broader model of bioaccumulation that incorporates these mechanisms. An improved mechanistic understanding of factors affecting tissue accumulation of legacy PFASs can inform management strategies for replacement compounds that exhibit similar properties. Many of the PFASs measured here will not degrade in the environment, and they have continued to be present in marine biota long after product phase-outs.[45] Understanding the mechanisms that drive the accumulation of PFASs in biological systems is critical for mitigating risks of legacy PFASs and predicting the future behavior of the much wider class of replacement compounds.

■ ASSOCIATED CONTENT

Supporting Information

The Supporting Information is available free of charge on the ACS Publications website at DOI: 10.1021/acs.estlett.9b00031.

Details of PFAS analysis, protein analysis, lipid analysis, statistical analysis, and relation to bioaccumulation, list of PFASs monitored, method detection limits, and summary statistics of measurements (PDF)

■ AUTHOR INFORMATION

Corresponding Author

*E-mail: cld292@mail.harvard.edu.

ORCID

Clifton Dassuncao: 0000-0001-7140-1344
Heidi Pickard: 0000-0001-8312-7522
Andrea K. Tokranov: 0000-0003-4811-8641
Miling Li: 0000-0001-8574-2625
Elsie M. Sunderland: 0000-0003-0386-9548

Notes

The authors declare no competing financial interest.

■ ACKNOWLEDGMENTS

The authors acknowledge financial support for this study from the National Institute of Environmental Health Sciences (P42ES027706) Superfund Research Center and the Smith Family Foundation. C.D. acknowledges a STAR graduate fellowship from the U.S. Environmental Protection Agency (F13D10739). The authors thank Maria Dam (Environment Agency, Faroe Islands) for assistance with pilot whale sample selection.

■ REFERENCES

(1) Toxicological Profile for Perfluoroalkyls. U.S. Department of Health and Human Services, Public Health Service: Atlanta, 2018.

(2) Sunderland, E. M.; Hu, X. C.; Dassuncao, C.; Tokranov, A. K.; Wagner, C. C.; Allen, J. G. A review of the pathways of human exposure to poly- and perfluoroalkyl substances (PFASs) and present understanding of health effects. *J. Exposure Sci. Environ. Epidemiol.* **2019**, *29*, 131.

(3) Kelly, B. C.; Ikonomou, M. G.; Blair, J. D.; Surridge, B.; Hoover, D.; Grace, R.; Gobas, F. A. P. C. Perfluoroalkyl Contaminants in an Arctic Marine Food Web: Trophic Magnification and Wildlife Exposure. *Environ. Sci. Technol.* **2009**, *43*, 4037−4043.

(4) Zhang, X.; Zhang, Y.; Dassuncao, C.; Lohmann, R.; Sunderland, E. M. North Atlantic Deep Water formation inhibits high Arctic contamination by continental perfluorooctanesulfonate discharges. *Global Biogeochem Cycles* **2017**, *31*, 1332−1343.

(5) Dassuncao, C.; Hu, X. C.; Nielsen, F.; Weihe, P.; Grandjean, P.; Sunderland, E. M. Shifting Global Exposures to Poly- and Perfluoroalkyl Substances (PFASs) Evident in Longitudinal Birth

DOI: 10.1021/acs.estlett.9b00031
Environ. Sci. Technol. Lett. 2019, 6, 119−125

Cohorts from a Seafood-Consuming Population. *Environ. Sci. Technol.* **2018**, *52*, 3738−3747.
(6) Arnot, J. A.; Gobas, F. A. P. C. A review of bioconcentration factor (BCF) and bioaccumulation factor (BAF) assessments for organic chemicals in aquatic organisms. *Environ. Rev. (Ottawa, ON, Can.)* **2006**, *14*, 257−297.
(7) Conder, J. M.; Hoke, R. A.; Wolf, W. d.; Russell, M. H.; Buck, R. C. Are PFCAs Bioaccumulative? A Critical Review and Comparison with Regulatory Criteria and Persistent Lipophilic Compounds. *Environ. Sci. Technol.* **2008**, *42*, 995−1003.
(8) Armitage, J. M.; Arnot, J. A.; Wania, F. Potential role of phospholipids in determining the internal tissue distribution of perfluoroalkyl acids in biota. *Environ. Sci. Technol.* **2012**, *46*, 12285−12286.
(9) Ng, C. A.; Hungerbuhler, K. Bioconcentration of perfluorinated alkyl acids: how important is specific binding? *Environ. Sci. Technol.* **2013**, *47*, 7214−7223.
(10) Shi, Y.; Vestergren, R.; Nost, T. H.; Zhou, Z.; Cai, Y. Probing the Differential Tissue Distribution and Bioaccumulation Behavior of Per- and Polyfluoroalkyl Substances of Varying Chain-Lengths, Isomeric Structures and Functional Groups in Crucian Carp. *Environ. Sci. Technol.* **2018**, *52*, 4592−4600.
(11) Greaves, A. K.; Letcher, R. J.; Sonne, C.; Dietz, R.; Born, E. W. Tissue-specific concentrations and patterns of perfluoroalkyl carboxylates and sulfonates in East Greenland polar bears. *Environ. Sci. Technol.* **2012**, *46*, 11575−11583.
(12) Ahrens, L.; Siebert, U.; Ebinghaus, R. Total body burden and tissue distribution of polyfluorinated compounds in harbor seals (Phoca vitulina) from the German Bight. *Mar. Pollut. Bull.* **2009**, *58*, 520−525.
(13) Armitage, J. M.; Arnot, J. A.; Wania, F.; Mackay, D. Development and evaluation of a mechanistic bioconcentration model for ionogenic organic chemicals in fish. *Environ. Toxicol. Chem.* **2013**, *32*, 115−128.
(14) Fujikawa, M.; Nakao, K.; Shimizu, R.; Akamatsu, M. The usefulness of an artificial membrane accumulation index for estimation of the bioconcentration factor of organophosphorus pesticides. *Chemosphere* **2009**, *74*, 751−757.
(15) Bittermann, K.; Spycher, S.; Endo, S.; Pohler, L.; Huniar, U.; Goss, K. U.; Klamt, A. Prediction of Phospholipid-Water Partition Coefficients of Ionic Organic Chemicals Using the Mechanistic Model COSMOmic. *J. Phys. Chem. B* **2014**, *118*, 14833−14842.
(16) Chen, F.; Gong, Z.; Kelly, B. C. Bioaccumulation Behavior of Pharmaceuticals and Personal Care Products in Adult Zebrafish (Danio rerio): Influence of Physical-Chemical Properties and Biotransformation. *Environ. Sci. Technol.* **2017**, *51*, 11085−11095.
(17) Droge, S. T. J. Membrane-water partition coefficients to aid risk assessment of perfluoroalkyl anions and alkyl sulfates. *Environ. Sci. Technol.* **2019**, *53*, 760−770.
(18) Fitzgerald, N. J. M.; Wargenau, A.; Sorenson, C.; Pedersen, J.; Tufenkji, N.; Novak, P. J.; Simcik, M. F. Partitioning and Accumulation of Perfluoroalkyl Substances in Model Lipid Bilayers and Bacteria. *Environ. Sci. Technol.* **2018**, *52*, 10433−10440.
(19) Weber, A. K.; Barber, L. B.; LeBlanc, D. R.; Sunderland, E. M.; Vecitis, C. D. Geochemical and Hydrologic Factors Controlling Subsurface Transport of Poly- and Perfluoroalkyl Substances, Cape Cod, Massachusetts. *Environ. Sci. Technol.* **2017**, *51*, 4269−4279.
(20) Zhang, X.; Lohmann, R.; Dassuncao, C.; Hu, X. C.; Weber, A. K.; Vecitis, C. D.; Sunderland, E. M. Source attribution of poly- and perfluoroalkyl substances (PFASs) in surface waters from Rhode Island and the New York Metropolitan Area. *Environ. Sci. Technol. Lett.* **2016**, *3*, 316−321.
(21) Bradford, M. M. A rapid and sensitive method for the quantitation of microgram quantities of protein utilizing the principle of protein-dye binding. *Anal. Biochem.* **1976**, *72*, 248−254.
(22) Folch, J.; Lees, M.; Stanley, G. H. S. A simple method for the isolation and purification of total lipids from animal tissues. *J. Biol. Chem.* **1956**, *226*, 497−509.
(23) Wang, J.; Pan, Y.; Cui, Q.; Yao, B.; Wang, J.; Dai, J. Penetration of PFASs Across the Blood Cerebrospinal Fluid Barrier and Its Determinants in Humans. *Environ. Sci. Technol.* **2018**, *52*, 13553−13561.
(24) Luebker, D. J.; Hansen, K. J.; Bass, N. M.; Butenhoff, J. L.; Seacat, A. M. Interactions of flurochemicals with rat liver fatty acid-binding protein. *Toxicology* **2002**, *176*, 175−185.
(25) Woodcroft, M. W.; Ellis, D. A.; Rafferty, S. P.; Burns, D. C.; March, R. E.; Stock, N. L.; Trumpour, K. S.; Yee, J.; Munro, K. Experimental characterization of the mechanism of perfluorocarboxylic acids' liver protein bioaccumulation: the key role of the neutral species. *Environ. Toxicol. Chem.* **2010**, *29*, 1669−1677.
(26) Zhang, L.; Ren, X. M.; Guo, L. H. Structure-based investigation on the interaction of perfluorinated compounds with human liver fatty acid binding protein. *Environ. Sci. Technol.* **2013**, *47*, 11293−11301.
(27) Hebert, P. C.; MacManus-Spencer, L. A. Development of a Fluorescence Model for the Binding of Medium- to Long-Chain Perfluoroalkyl Acids to Human Serum Albumin Through a Mechanistic Evaluation of Spectroscopic Evidence. *Anal. Chem.* **2010**, *82*, 6463−6471.
(28) MacManus-Spencer, L. A.; Tse, M. L.; Hebert, P. C.; Bischel, H. N.; Luthy, R. G. Binding of perfluorocarboxylates to serum albumin: a comparison of analytical methods. *Anal. Chem.* **2010**, *82*, 974−981.
(29) Bischel, H. N.; Macmanus-Spencer, L. A.; Zhang, C.; Luthy, R. G. Strong associations of short-chain perfluoroalkyl acids with serum albumin and investigation of binding mechanisms. *Environ. Toxicol. Chem.* **2011**, *30*, 2423−2430.
(30) Dauchy, X.; Boiteux, V.; Bach, C.; Rosin, C.; Munoz, J. F. Per- and polyfluoroalkyl substances in firefighting foam concentrates and water samples collected near sites impacted by the use of these foams. *Chemosphere* **2017**, *183*, 53−61.
(31) Houtz, E. F.; Sutton, R.; Park, J. S.; Sedlak, M. Poly- and perfluoroalkyl substances in wastewater: Significance of unknown precursors, manufacturing shifts, and likely AFFF impacts. *Water Res.* **2016**, *95*, 142−149.
(32) Houtz, E. F.; Sedlak, D. L. Oxidative conversion as a means of detecting precursors to perfluoroalkyl acids in urban runoff. *Environ. Sci. Technol.* **2012**, *46*, 9342−9349.
(33) Nouhi, S.; Ahrens, L.; Campos Pereira, H.; Hughes, A. V.; Campana, M.; Gutfreund, P.; Palsson, G. K.; Vorobiev, A.; Hellsing, M. S. Interactions of perfluoroalkyl substances with a phospholipid bilayer studied by neutron reflectometry. *J. Colloid Interface Sci.* **2018**, *511*, 474−481.
(34) Wang, X.; Li, B.; Zhao, W. D.; Liu, Y. J.; Shang, D. S.; Fang, W. G.; Chen, Y. H. Perfluorooctane sulfonate triggers tight junction "opening" in brain endothelial cells via phosphatidylinositol 3-kinase. *Biochem. Biophys. Res. Commun.* **2011**, *410*, 258−63.
(35) Berntsen, H. F.; Bjorklund, C. G.; Audinot, J. N.; Hofer, T.; Verhaegen, S.; Lentzen, E.; Gutleb, A. C.; Ropstad, E. Time-dependent effects of perfluorinated compounds on viability in cerebellar granule neurons: Dependence on carbon chain length and functional group attached. *NeuroToxicology* **2017**, *63*, 70−83.
(36) Eggers Pedersen, K.; Basu, N.; Letcher, R.; Greaves, A. K.; Sonne, C.; Dietz, R.; Styrishave, B. Brain region-specific perfluoroalkylated sulfonate (PFSA) and carboxylic acid (PFCA) accumulation and neurochemical biomarker responses in east Greenland polar bears (Ursus maritimus). *Environ. Res.* **2015**, *138*, 22−31.
(37) Ng, C. A.; Hungerbuhler, K. Bioaccumulation of perfluorinated alkyl acids: observations and models. *Environ. Sci. Technol.* **2014**, *48*, 4637−4648.
(38) Bittermann, K.; Linden, L.; Goss, K. U. Screening tools for the bioconcentration potential of monovalent organic ions in fish. *Environ. Sci: Processes Impacts* **2018**, *20*, 845−853.
(39) Goss, K. U.; Bittermann, K.; Henneberger, L.; Linden, L. Equilibrium biopartitioning of organic anions - A case study for humans and fish. *Chemosphere* **2018**, *199*, 174−181.

DOI: 10.1021/acs.estlett.9b00031
Environ. Sci. Technol. Lett. 2019, 6, 119−125

(40) Matyszewska, D.; Tappura, K.; Orädd, G.; Bilewicz, R. Influence of perfluorinated compounds on the properties of model lipid membranes. *J. Phys. Chem. B* **2007**, *111*, 9908−9918.
(41) Nakagawa, H.; Hirata, T.; Terada, T.; Jutabha, P.; Miura, D.; Harada, K. H.; Inoue, K.; Anzai, N.; Endou, H.; Inui, K. I.; Kanai, Y.; Koizumi, A. Roles of organic anion transporters in the renal excretion of perfluorooctanoic acid. *Basic Clin. Pharmacol. Toxicol.* **2008**, *103*, 1−8.
(42) Weaver, Y. M.; Ehresman, D. J.; Butenhoff, J. L.; Hagenbuch, B. Roles of rat renal organic anion transporters in transporting perfluorinated carboxylates with different chain lengths. *Toxicol. Sci.* **2010**, *113*, 305−314.
(43) Yang, C. H.; Glover, K. P.; Han, X. Organic anion transporting polypeptide (Oatp) 1a1-mediated perfluorooctanoate transport and evidence for a renal reabsorption mechanism of Oatp1a1 in renal elimination of perfluorocarboxylates in rats. *Toxicol. Lett.* **2009**, *190*, 163−171.
(44) Zhao, W.; Zitzow, J. D.; Ehresman, D. J.; Chang, S. C.; Butenhoff, J. L.; Forster, J.; Hagenbuch, B. Na+/Taurocholate Cotransporting Polypeptide and Apical Sodium-Dependent Bile Acid Transporter Are Involved in the Disposition of Perfluoroalkyl Sulfonates in Humans and Rats. *Toxicol. Sci.* **2015**, *146*, 363−373.
(45) Dassuncao, C.; Hu, X. C.; Zhang, X.; Bossi, R.; Dam, M.; Mikkelsen, B.; Sunderland, E. M. Temporal Shifts in Poly- and Perfluoroalkyl Substances (PFASs) in North Atlantic Pilot Whales Indicate Large Contribution of Atmospheric Precursors. *Environ. Sci. Technol.* **2017**, *51*, 4512−4521.

DOI: 10.1021/acs.estlett.9b00031
Environ. Sci. Technol. Lett. 2019, 6, 119−125